Ocean Environment Sensing using Polarimetric and Interferometric SAR

D. Schuler, M. Sletten,
T. Ainsworth, J.S. Lee
Code 7260
Naval Research Laboratory
4555 Overlook Ave. SW
Washington DC 20375
dschuler@ccs.nrl.navy.mil

S. Frasier
Electrical and Computer Eng. Dept.
University of Massachusetts
Amherst, MA 01003
frasier@ecs.umass.edu

B. Holt
MS 300-323
Jet Propulsion Lab
4800 Oak Grove Dr.
Pasadena, CA, 91109
ben@pacific.jpl.nasa.gov

***Abstract*-New methods have been investigated which use fully polarimetric synthetic aperture radar (POLSAR) image data to measure ocean wave slopes. Independent techniques have been developed to measure wave slope spectra in both the radar azimuth and range directions. Wave spectra measured using the new methods are compared with spectra developed using conventional SAR intensity-based methods, and with spectra from in situ buoys. Wave-current interactions may also be measured using the same measurement techniques [1]. NASA/JPL/AIRSAR L-band image data from California coastal waters and from the New York Bight are used in the studies.**

NRL has also recently lead two collaborative field experiments that feature Along-Track Interferometric SAR (AT-INSAR) systems. In April, 2003, NRL, NASA JPL and UCLA collaborated in a study of sub-mesoscale coastal eddies that featured the NASA/JPL/AIRSAR. NRL has also recently collaborated with the University of Massachusetts in a deployment of their Dual Beam Interferometer on the west coast of Florida. This paper presents preliminary data from both of these experiments.

I. POLSAR MEASUREMENT OF OCEAN WAVE SLOPES

Synthetic aperture radar images of ocean surface waves have been used with intensity-based algorithms to measure physical parameters such as wave slope spectra [2]. SAR instruments operating at a single polarization base their measurements on wave-induced backscatter cross-section modulations. These measurements require a parametrically complex modulation transfer function (MTF) to relate wave properties to the SAR measurements. The studies reported here investigate the feasibility of using polarimetric SAR (POLSAR) data to measure ocean wave slopes in both the radar azimuth and range directions. In the Fourier-transform domain, this orthogonal slope information may be used to estimate a complete directional ocean wave slope (or height) spectrum. Motion-induced "velocity-bunching" effects still present difficulties for wave measurements in the azimuth direction. The advantage of using these new POLSAR algorithms is, however, that a nearly direct physical measurement of the slope is made which does not require the use of a nonlinear, complex MTF.

Modulations of the polarization orientation angle θ are largely caused by waves traveling in the azimuth direction. A method [3] that senses modulations of θ is used to measure wave slopes in the azimuth direction. Slopes smaller than 1^o are measurable by this method. An eigenvector/eigenvalue decomposition parameter alpha described in [4] is used to measure wave slopes in the orthogonal range direction. Waves in the range direction cause modulation of the local incidence angle that, in turn, also modulate the value of alpha. From these azimuth and range slope pairs, a complete directional wave spectrum may be estimated. Measurements of θ can also be used to study ocean wave-current interactions such as those produced by internal waves [1].

NASA/JPL/AIRSAR L - band ocean scatter data has been used in the studies. Comparisons will be made of ocean wave spectra measured using this new POLSAR method, spectra produced from intensity images, and conventional National Data Buoy Center (NDBC) buoy spectra.

A. Orthogonal Slope Measurement Pairs

It has been shown by Schuler et al [3] that by measuring the orientation angle shift in the polarization signature one may determine a combined effect of the surface tilts. In particular, the shift in the orientation angle is related to the azimuth/range surface tilts and the local incidence angle. This relationship, derived by Lee [4] and Pottier [5] is:

$$\tan\,\theta = \frac{\tan\,\omega}{\sin\,\phi - \tan\,\gamma\,\cos\,\phi} \qquad (1)$$

where, θ, $\tan\omega$, $\tan\gamma$, and ϕ are the shift in the orientation angle, the azimuth slope, the ground range slope, and the radar incidence angle, respectively. According to (1), the azimuth tilts may be estimated from the shift in the orientation angle if the range tilt is known. The orthogonal range slope can be estimated using the value of local incidence angle associated with alpha for each pixel. Since for the ocean surface, the tilt angles are small, the denominator in (1) may be approximated by $\sin\phi$. Thus, for the ocean surface, the azimuth slope may be written as $\tan\omega \approx (\sin\phi)\cdot\tan\theta$. Knowledge of the azimuth slope, $\tan\omega$ and the range slope $\tan\gamma$ provides complete slope information for each image pixel.

1) Orientation Angle Measurements: Azimuth Direction Wave Spectra

POLSAR data is represented, for single-look complex data, by a scattering matrix. Single-look complex, or multi-look complex data, is represented by a covariance (or coherency) matrix. An orientation angle shift causes rotation of all these matrices about the line of sight. Since the orientation angle information is embedded in the POLSAR data, several methods have been developed to estimate azimuth slope induced orientation angles for the land and sea. The "polarization signature" method and the "circular polarization" methods have proven to be the two most effective. A complete discussion of these methods and the relation of the orientation angle to orthogonal slopes and radar parameters are given in Lee *et al*. [4]. AIRSAR data (1994) at L-band imaging a coastal area near the Gualala River in northern California was

Report Documentation Page

Form Approved
OMB No. 0704-0188

1. REPORT DATE	2. REPORT TYPE	3. DATES COVERED
01 SEP 2003	**N/A**	**-**

4. TITLE AND SUBTITLE	5a. CONTRACT NUMBER
Ocean Environment Sensing using Polarimetric and Interferometric SAR	5b. GRANT NUMBER
	5c. PROGRAM ELEMENT NUMBER
6. AUTHOR(S)	5d. PROJECT NUMBER
	5e. TASK NUMBER
	5f. WORK UNIT NUMBER
7. PERFORMING ORGANIZATION NAME(S) AND ADDRESS(ES) **Naval Research Laboratory 4555 Overlook Ave. SW Washington DC 20375**	8. PERFORMING ORGANIZATION REPORT NUMBER
9. SPONSORING/MONITORING AGENCY NAME(S) AND ADDRESS(ES)	10. SPONSOR/MONITOR'S ACRONYM(S)
	11. SPONSOR/MONITOR'S REPORT NUMBER(S)

12. DISTRIBUTION/AVAILABILITY STATEMENT
Approved for public release, distribution unlimited

13. SUPPLEMENTARY NOTES
See also ADM002146. Oceans 2003 MTS/IEEE Conference, held in San Diego, California on September 22-26, 2003. U.S. Government or Federal Purpose Rights License., The original document contains color images.

14. ABSTRACT

15. SUBJECT TERMS

16. SECURITY CLASSIFICATION OF:			17. LIMITATION OF ABSTRACT	18. NUMBER OF PAGES	19a. NAME OF RESPONSIBLE PERSON
a. REPORT	b. ABSTRACT	c. THIS PAGE			
unclassified	**unclassified**	**unclassified**	**UU**	**6**	

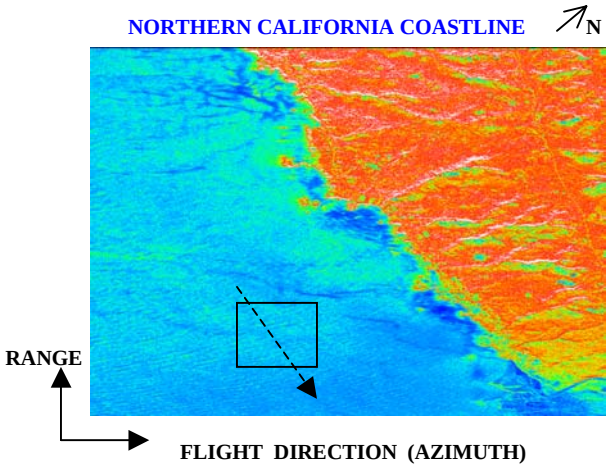

Fig. 1. An L-band, VV – pol, AIRSAR image showing ocean waves propagating through the study area box.

used to determine if the azimuth component of an ocean wave spectrum could be measured using orientation angle modulation. Fig. 1 is an L-band, VV-pol, image that shows the coastal area and the measurement study site. A wave system with an estimated dominant wavelength of 156m is propagating through the site with a wind/wave direction of 320^o (NDBC Buoy, Bodega Bay). Modulations in the polarization orientation angle induced by azimuth traveling ocean waves in the study area are shown in Fig. 2a) and a histogram of the orientation angles is given in Fig. 2b). Fig. 3 gives an orientation angle spectrum for waves in the study area. Fig.4(a-b) gives plots of spectral intensity vs wavenumber a) for wave-induced orientation modulations and, b) VV-pol intensity modulations in the direction of maximum spectral energy.

2) Alpha Parameter Measurements: Range Direction Wave Spectra

An independent concept has been developed for POLSAR measurements of ocean slopes in the range direction. This technique was created as a means of circumventing difficulties associated with conventional backscatter intensity-based methods.

The alpha (α) parameter, developed from the Cloude-Pottier <<H/A/α>> polarimetric decomposition theorem [5], has desirable

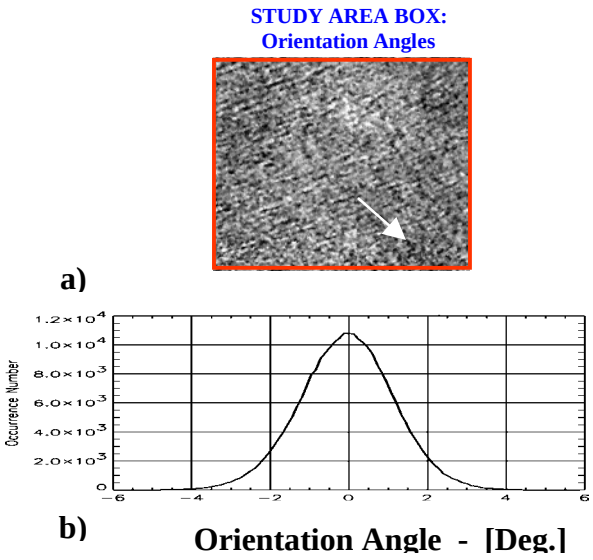

Fig. 2(a-b). a) Modulations in the orientation angle, θ, and, b) a histogram of the distribution of study-area θ values.

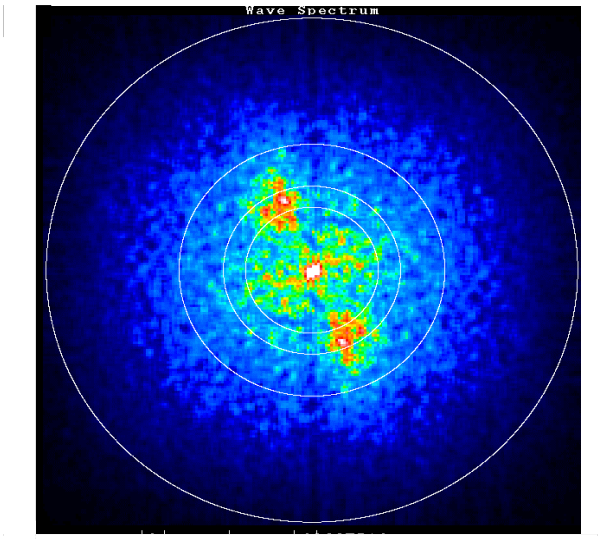

Fig. 3. Orientation angle spectra vs. wavenumber for azimuth direction waves propagating in the study area. The white rings correspond to 50m, 100m, 150m and 200m. The dominant wave is propagating at a heading of 315^o.

properties: 1) It is roll-invariant in the azimuth direction and, 2) in the range direction it is sensitive to wave-induced modulations ($\delta\phi$) in the local incidence angle ϕ. Thus, the measurements are well de-coupled. Model studies [5] resulted in an estimate of what the parametric relation, α vs. incidence angle ϕ, should be for an assumed Bragg-scatter model. The sensitivity (i.e., the slope of the curve of $\alpha(\phi)$) was large enough to warrant study using real POLSAR ocean backscatter data. A curve of α vs. incidence angle ϕ was measured for the 1994 Gualala River AIRSAR data. This curve had low noise, a high sensitivity for the slope of α (ϕ), and

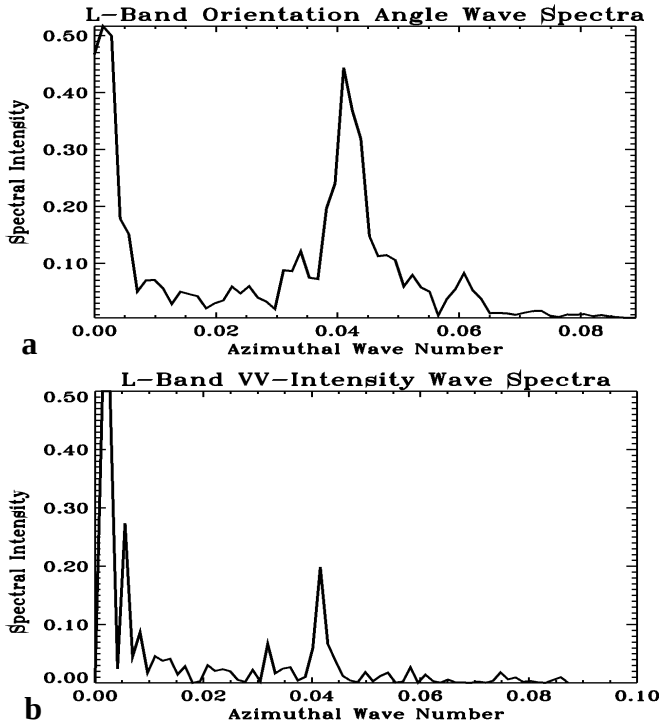

Fig. 4 (a-b). Plots of spectral intensity vs. wavenumber, a) for wave-induced orientation angle modulations, and b) conventional VV-pol intensity modulations.

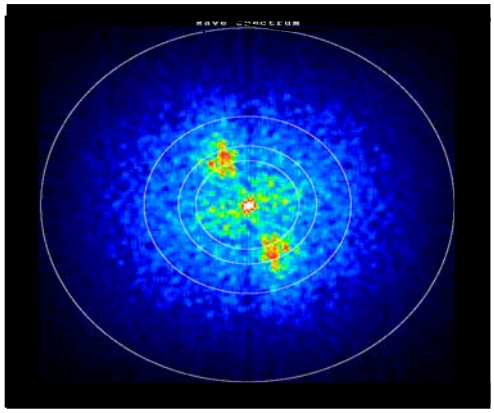

Fig.5. Spectrum of waves in the range direction obtained using the alpha parameter decomposition method.

could be related to the range slope.

Wave spectra may be developed using the alpha parameter. An image of the study area is first formed with the mean of α (ϕ) removed line by line in the range direction. An FFT of the study area then results in a wave spectra (Fig. 5) that correlates in form and direction with the spectrum of Fig. 3. The spectrum of Fig. 5 is an alpha parameter spectrum. This spectrum can easily be converted to a range wave slope spectrum.

B. Internal Wave Measurements

The use of polarimetric SAR to measure changes in wave slope distributions caused by internal waves has also been investigated. AIRSAR L-band data on internal waves was used from the 1992 Joint US/Russia Internal Wave Remote Sensing Experiment (JUSREX'92) in the New York Bight. Extensive sea-truth is

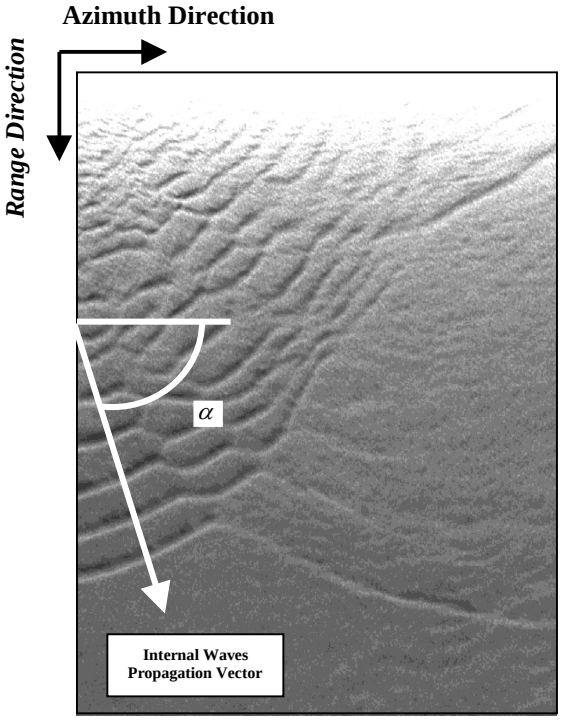

Fig. 6: AIRSAR L-band VV-pol image of internal wave intersecting packets in the New York Bight. Arrow indicates propagation direction for the chosen packet. The angle α relates the SAR and internal wave coordinates.

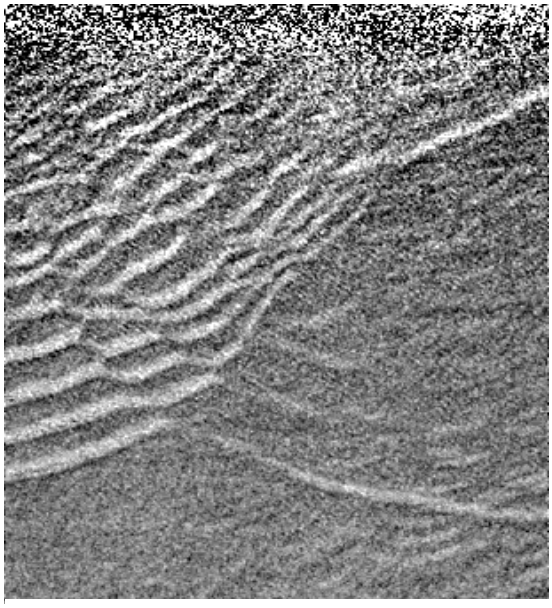

Fig. 7. Orientation angle image of the internal wave packets in the New York Bight.

available for this experiment.

An AIRSAR VV-polarization image of several interacting internal wave packets is given in Fig. 6. Wave-current interactions make the wave slope distributions asymmetric in the propagation direction (parallel to the current flow). An image of orientation angle perturbations caused by the internal waves is given in Fig. 7. The changes in orientation angle for the internal waves of Fig. 6 may be observed as lighter stripes in Fig.7. The orientation angle values obtained along the propagation vector line (Fig. 6) are given in Fig. 8. Averaging in the direction orthogonal to the propagation vector was 25 pixels. The current-induced asymmetry creates a mean slope that is, in turn, manifested as a change in the orientation angle. The relation between the orientation angle slope, wave slopes in the radar azimuth and range directions ($\tan\omega$, $\tan\gamma$),

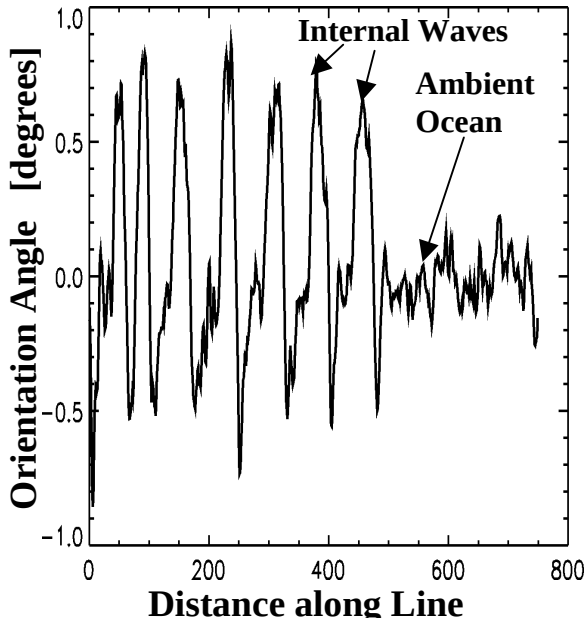

Fig. 8. Orientation angle values along the propagation vector for the internal wave packets.

and the radar look angle ϕ is given by (1), and the average $\langle \tan\theta \rangle$ is:

$$\langle \tan\theta \rangle = \int_{-\infty}^{\infty} \tan\theta(\omega,\gamma) P(\omega,\gamma) d\gamma d\omega \qquad (2)$$

where, *P* is the joint probability distribution function for the surface slopes in the azimuth and range directions. If the slopes are zero-meaned but *P* is skewed, then the mean orientation angle may not be zero even though the mean azimuth and range slopes are zero. The internal waves are visible in Fig. 7 precisely for this reason. It is apparent from the above equation, that the both the range and the azimuth slopes have an effect on the mean orientation angle. If the intermediate wavelength waves are modulated by the internal wave, then both slopes will change locally. This will yield a non-zero mean orientation angle. For the JUSREX'92 conditions these perturbations become significantly larger for wavelengths longer than 0.6m and shorter than 25m. The mean square slope $< \beta^2 >$ of these perturbed waves was calculated as 1.72 ^{o}.

II. RECENT SAR/AT-INSAR INVESTIGATIONS

A. AIRSAR Study of Coastal Eddies in the Southern California Bight

In April, 2003, NRL, JPL, and UCLA collaborated in an AIRSAR-based investigation of sub-mesoscale eddies in the Southern California Bight, the region of the coastal Pacific Ocean that extends west from Los Angeles and south from Santa Barbara. Spiral patterns in surfactant slicks with diameters in the 5-10 km range have been studied previously in this area using satellite-based radars [6], and are in fact observed in radar and sun-glint imagery of most of the world's oceans [7]. It is believed that these spirals are produced by sub-mesoscale oceanic eddies, although the generation mechanism for eddies on this scale is not yet understood. In order to gain important clues as to the spiral's generation mechanism, AIRSAR was used to capture their spatial and temporal evolution, information that cannot be obtained with the long repeat-pass times provided by a satellite-based radar.

AIRSAR was used in both POLSAR and AT-INSAR modes in this investigation, the latter in order to estimate the surface currents associated with these oceanic features. In an AT-INSAR system, data is collected simultaneously on two independent channels that are fed by two separate receiving antennas. These two antennas are displaced from one another along the axis of the aircraft. This arrangement allows two independent, time-separated SAR images of the scene of interest to be generated. The antenna spacing and the velocity of the aircraft determine the value of the time separation. By forming an interferogram with these two complex images, the radial component of the surface velocity can be measured. When used to image the ocean surface, this surface *velocity* measurement can be converted into a surface *current* estimate. [See, for example, Ref. 8]

An example of the single-channel imagery collected during this campaign is shown in Fig. 9. (At the time this paper was written, AT-INSAR imagery was not yet available.) This is a preliminary mosaic formed by joining overlapping passes of survey (i.e., unfocussed) imagery. The frequency is L-band and the polarization vertical. A chain of three spiral patterns can be observed off the western end of Santa Catalina Island, (visible at the bottom of the figure), with the central spiral being the most visible. A five-hour time-sequence of precision (i.e., fully focussed) images is currently being produced and analyzed in order to determine the spatial/temporal evolution of these spirals and the associated surface currents. The latter will be deduced through a combination of AT-INSAR processing and image-to-image slick tracking.

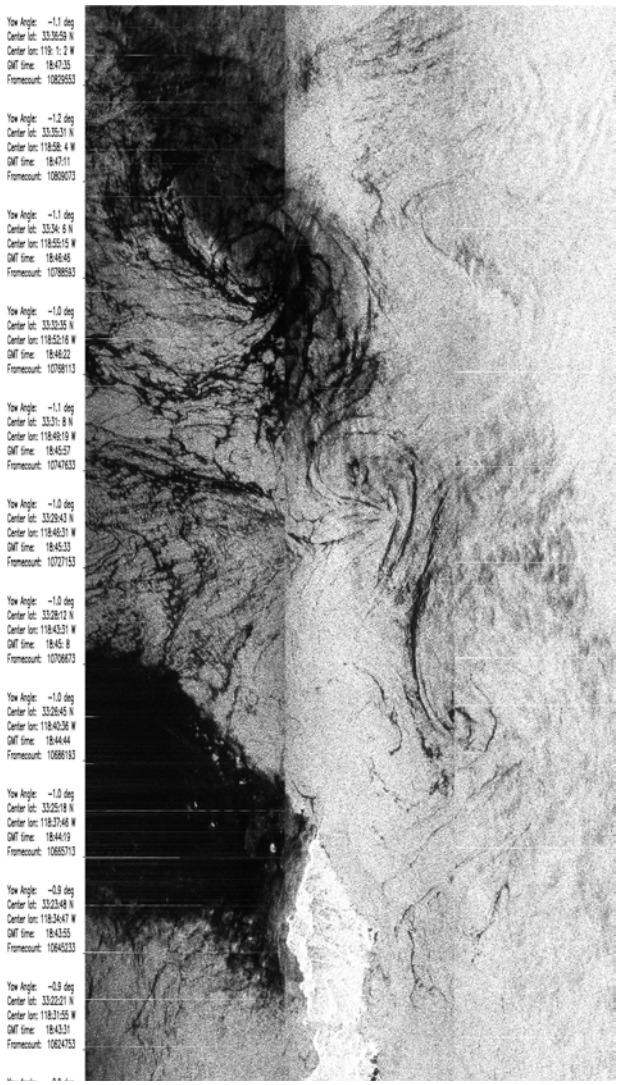

Fig. 9 Mosaic of AIRSAR L-VV images showing spiral slick patterns in the Southern California Bight near Santa Catalina Island. The image dimensions are approximately 50 km x 25 km.

B. Deployment of the U-MA Dual Beam Interferometer

In December, 2002, NRL and the University of Massachusetts-Amherst (UMA) collaborated in the deployment of the UMA Dual Beam Interferometer (DBI) [8] on a NOAA P3 aircraft. The DBI is a unique AT-INSAR system that requires only a *single* aircraft pass to generate a *vector* estimate of the surface current velocity. This capability comes about through the use of two independent AT-INSARs, one directed 20° forward of broadside, the other 20° aft. By combining the two radial velocity estimates provided by these two interferometers, a vector velocity measurement can be made.

The DBI is a vertically-polarized system that operates at 5.3 GHz and has a spatial resolution of up to 7.5 m. All system components except a laptop computer are housed in a P3 wing pod. Communication with the pod from within the main aircraft cabin is achieved using a wireless local area network and a laptop computer.

Fig. 10 shows one of the first DBI images, collected over Charlotte Harbor, northwest of Ft. Myers, FL. Both forward-

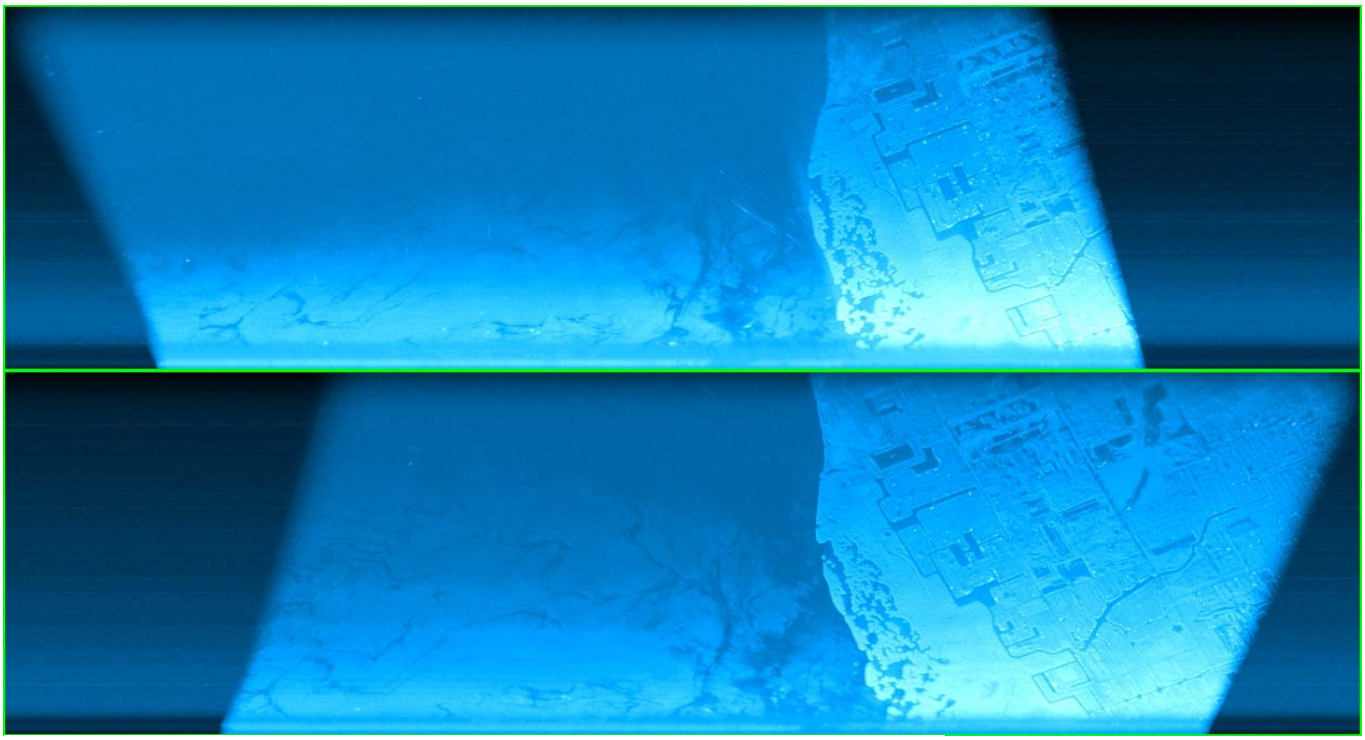

Fig. 10. Forward- (bottom) and aft-looking (top) DBI images of Charlotte Harbor, near Ft. Meyers FL.

(lower) and aft-looking (upper) images are shown. Given the very low surface winds present on this particular day, the flight altitude was lowered to approximately 600 m from its nominal value of 1000 m. The swath corresponds to incidence angles between 69° and 86° and the swath width is approximately 7 km with a range resolution of 16.7 m. Images were focused using an adaptation of the extended chirp scaling algorithm [9] implemented by NRL. Range and azimuth resolution are approximately matched with 66 independent looks.

Surface slick features are observable in the images over much of the water surface within the bay. Such features are commonly observable under light surface winds and are often attributed to biological sources. However, a distinct difference in ocean backscatter intensity exists between the forward and aft looks, with features on the ocean surface more distinct in the forward look. Given the similar intensities of land echoes, it is likely that these differences are a consequence of the directional spectrum of Bragg resonant surface waves.

Due to overheating within the wing pod, only one of the two data acquisition modules was operating during the flights in December 2002. This prevented collection of the data necessary to form an interferogram. Since that time, vents have been added to the wing pod to alleviate this problem. Additional test flights are scheduled for June, 2003 at which time the full interferometric capability of the system will be demonstrated.

III. CONCLUSIONS

Methods have been investigated which are capable of measuring ocean slopes. Wave slope spectra and slope distributions can be measured. Wave-current interactions associated with internal waves may also be studied. SAR motion-related problems, such as velocity-bunching, can be solved using iterative algorithms similar to those previously developed. The new measurements are sensitive and provide nearly direct measurements of ocean slopes.

Two recent deployments of AT-INSAR systems were described. In the first, NRL, NASA/JPL, and UCLA collaborated in a JPL/AIRSAR-based investigation of sub-mesoscale eddies in the Southern California Bight. Surface current estimates derived from AT-INSAR data collected during this deployment should help develop an understanding of the generation mechanism for these eddies. In the second, NRL and U-MA collaborated in the first deployment of the U-MA DBI system. Tests scheduled for June, 2003 should demonstrate the ability of this system to measure the *vector* surface velocity field.

REFERENCES

[1] D. Schuler, D. Kasilingam, and J.S. Lee, " Slope Measurements of Ocean Internal Waves and Current Fronts using Polarimetric SAR", Proceedings of the European Conference on Synthetic Aperture radar (EUSAR-2002), Cologne, Germany, 4-6 June, 2002.

[2] W. Alpers and C.L. Rufenach, "On the detectability of ocean surface waves by real and synthetic aperture radar", *J. Geophys. Res*., vol. 86, pp. 6481-6498, 1981.

[3] D.L. Schuler, J.S. Lee, and G. De Grandi, "Measurement of topography using polarimetric SAR images", *IEEE Transactions on Geosci. and Remote Sens.*, vol. 34, pp 1266-1277 (1996).

[4] J.S. Lee, D.L. Schuler, T.L. Ainsworth, "Polarimetric SAR data compensation for terrain azimuth slope variation", *IEEE Trans. Geosci. Remote Sens.*, 2000, 38, pp. 2153-2163.

[5] E. Pottier, "Unsupervised classification scheme and topography derivation of POLSAR data on the <<H/A/α>> polarimetric decomposition theorem", in *Proc. of the 4th International Workshop on Radar Polarimetry*, IRESTE, Nantes, France, pp. 535-548.

[6] P. DiGiacomo, and B. Holt, "Satellite observations of small coastal ocean eddies in the Southern California Bight", *J. Geophys. Res*., vol. 106, pp. 22,521-22,543

[7] W..Munk, L. Armi, K. Fischer, and F. Zachariasen, "Spirals on the sea", *Proc. R. Soc. Lond. A*, vol. 456, pp. 1217-1280. 2000.

[8] S.J. Frasier, and A. J. Camps, "Dual-Beam Interferometry for Ocean Surface Current Vector Mapping", *IEEE Trans. Geosci. Remote Sens*., vol. 39, no. 2, Feb. 2001.

[9] A. Moriera and Y. Huang, "Airborne SAR Processing of Highly Squinted Data Using a Chirp Scaling Approach with Integrated Motion Compensation", *IEEE Trans. Geosci. Remote Sens*., vol. 32, no. 5, Sept. 1994.